FATIGUE BEHAVIOUR OF ANGLE-PLY GFRP LAMINATES: EXPERIMENTAL AND ANALYSIS METHODOLOGY TO EVALUATE TIME- AND CYCLE-DEPENDENT PROPERTIES

Seyed Shayan Khalooei Tafti, Anastasios P. Vassilopoulos

Composite Construction Laboratory (CCLab), École Polytechnique Fédérale de Lausanne, Lausanne, CH (shayan.khalooei@epfl.ch)

Abstract: *The tension-tension fatigue behavior of angle-ply GFRP laminate is studied in this work. The main objective is to develop an efficient methodology to obtain time- and cycle-dependent properties considering their interaction. Different aspects of time-dependent deformation on fatigue behavior are discussed. The S-N curves are adjusted according to the true stress state resulting from large creep deformation under fatigue loading. Moreover, the effect of fiber orientation on fatigue stiffness evolution is investigated. A simple analysis is performed to exclude the stiffening effect due to fiber orientation from the monitored fatigue stiffness evolution, which provides the fatigue stiffness evolution due to pure fatigue damage. An experimental methodology is proposed for time-dependent properties to evaluate the effect of fatigue damage on viscoelastic properties. DMA experiments were used to obtain the time-dependent properties of the fatigue-damaged specimen. Finally, this work presents the feasibility of extending the time-temperature superposition principle to time-temperature-fatigue damage superposition, aiming to predict the viscoelastic properties depending on the fatigue damage level.*

Keywords: Fatigue, composites, Creep-fatigue interaction; Residual stiffness; DMA; TTSP.

1. Introduction

Polymer matrix composites are widely used in numerous engineering fields such as aerospace, wind energy, automotive, and civil engineering as a primary component due to their high specific strength and stiffness. Engineering structures experience different loading types, such as creep, fatigue, and impact, during their lifetime. Nowadays, it is widely accepted that FRP composite's long-term behavior should be evaluated for their application in different engineering domains, especially in load-bearing parts of structures. Investigation of FRP composites' fatigue and creep behavior has already been examined since the 1940s, when these materials were firstly introduced in different engineering applications [1, 2]. Since the polymeric matrices possess inherent viscoelastic properties, they are expected to show time-dependent viscoelastic behavior. Therefore, the viscoelastic behavior of polymeric matrices used in structural components can significantly affect FRP composites' failure response under loading. Due to this inherent viscoelastic nature of polymer matrix composite, time-dependent phenomena such as creep, recovery, and relaxation should be considered to evaluate composite laminates' long-term behavior.

In most of the works that already exist in the literature, creep and fatigue behavior have been studied separately for FRP composites' long-term behavior. However, the FRP composite materials undergo time-dependent deformation (creep deformation) even under constant

amplitude (CA) fatigue loading with non-zero mean stress. Therefore, under fatigue loading, time-dependent behavior would affect the cycle-dependent properties and the 'materials' response, e.g., strength, stiffness, and failure modes. As a result, FRP composites' viscoelastic behavior should be considered for accurate evaluation and prediction of cycle-dependent properties. On the other side, investigation of the effect of fatigue damage on the viscoelastic properties could be more challenging as reported in many works in the literature, i.e., some related research reviewed in [2]. There is a lack of an efficient methodology to investigate the evolution of viscoelastic properties during fatigue loading. The available experimental methodologies to obtain the viscoelastic properties, like those described in [3, 4] suggesting the application of an Interrupted creep-fatigue loading pattern, can affect the fatigue behavior and lifetime of GFRP composites. Therefore, the fatigue life prediction models proposed in the literature, considering the viscoelastic behavior, are developed using the time-dependent properties of undamaged material, directly obtained by conducting creep tests [5].

Based on the challenges discussed above, this work aims to study the fatigue behavior of GFRP composites considering both time- and cycle-dependent behavior as well as their interaction. For this purpose, a robust experimental and analysis methodology is presented to investigate the creep-fatigue interaction under fatigue loading. Angle ply $[\pm 45]_{2s}$ GFRP laminates have been fabricated and used in this work to discuss the presented methodology's performance. Quasi-static experiments have been performed to obtain the GFRP laminate's mechanical properties, i.e., ultimate strength and stiffness, while CA fatigue experiments were performed under different maximum stress levels and three *R*-ratios of 0.1, 0.5, and 0.8 to investigate the material's fatigue performance. The DIC method has been used for strain measurements as well as for studying comparatively the distribution and evolution of the fatigue damage under different loading conditions. The Dynamic Mechanical Analysis (DMA) was used to obtain the viscoelastic properties of damaged material (cut from failed specimen) as well as properties of undamaged ones. The creep master curves were obtained by adopting the time-temperature superposition principle (TTSP) and conducting short-term creep tests at several temperatures [6]. The feasibility of using TTSP on a damaged specimen under fatigue loading was studied based on the limited DMA tests performed and presented in this work. As a result, this work can potentially introduce an extension to the TTSP, the "time-temperature-fatigue damage superposition principle" (TTFDSP). The analysis part is also separated to discuss the evolution of cycle- and time-dependent properties. The effect of relatively large strain resulting from viscoelastic behavior has been addressed for cycle-dependent properties. The effect of fiber-reorientation, which results from the creep deformation, has been also studied. The fiber reorientation during loading was obtained using the DIC measurements for longitudinal and transverse strain. Accordingly, a simple analysis based on the classical laminate theory (CLT) is proposed to exclude the effect of fiber reorientation's stiffness increase [7]. For time-dependent properties, the results obtained by DMA tests on the fatigue-damaged sample were compared to the undamaged one to illustrate the effect of fatigue on viscoelastic properties. In the last part, the DIC results for different stress levels and *R*-ratios are presented to comparatively discuss the damage distribution and evolution for different loading conditions.

2. Experimental procedure

2.1 Material fabrication and test setup

Unidirectional E-glass fiber fabrics (EC 9-68) with an area density of 425 gr/m^2 and ply thickness of 0.45 mm were impregnated by the low viscosity resin, Biresin® CR83, mixed with the hardener Sika CH83-2, in the ratio of 10:3, to fabricate the $[\pm 45]_{2s}$ GFRP laminates. As depicted in Figure 1-a, the vacuum infusion method was used to fabricate GFRP laminates with dimensions of 40×40 cm^2 using a vacuum pump with a pressure of 0.95 bar. The laminate was kept in the vacuum for 24 hours at laboratory conditions (22±2 °C, 40±10 % RH) and afterward was put in an oven at 70°C for 8 hours for post-curing. Specimens with 250 × 25 mm^2 (length × width) were cut from the laminates by a water-jet cutting machine, and two aluminum tabs with the dimensions of 40 × 25 mm^2 were glued to each specimen end, according to the ASTM D3039. Specimens have been sprayed to make speckle patterns for DIC measurements, as illustrated in Figure 1-b. The Quasi-static and CA fatigue experiments were conducted at an Instron 8800 hydraulic universal testing rig of 100-kN capacity with an accuracy of ±0.01 kN. The test setup for CA fatigue experiments is shown in Figure 1-c. For DIC measurements, a camera Point Grey - Grasshopper3 with a resolution of 2.2 Mpixels and a Fujinon HF35SA-1 35mm F/1.4 lens are used. An infrared (IR) thermal camera with an accuracy of 0.1°C and optical resolution of 160x120 pixels was also employed during the fatigue experiments to record the evolution of the specimen's surface temperature.

2.2 Quasi-static and fatigue Tests

Quasi-static tests have been conducted on several samples to obtain the ultimate tensile strength of material with the same loading rate as fatigue tests. Based on the static results, different maximum stress levels are considered for CA tests. Fatigue tests have been conducted under three *R*-ratios of 0.1, 0.5 and 0.8 considered. The loading rate of 10 kN/sec was chosen to avoid significant self-generated temperature.

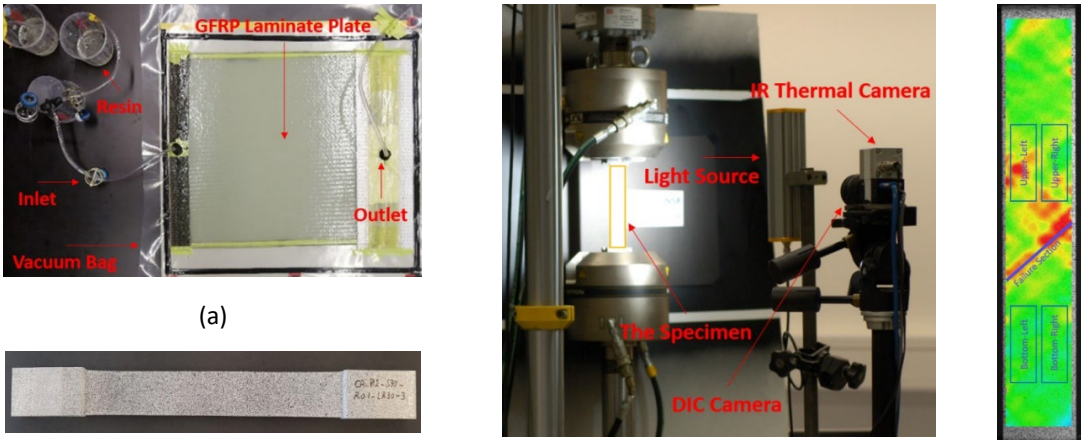

(a) (b) (c) (d)

Figure 1. (a) Fabrication Process (Vacuum Infusion), (b) Sprayed specimen for DIC, (c) Fatigue test setup, (d) Cutting sample for DMA tests based on DIC results

2.3 DMA experiments

The DMA experiments were performed using a TA Instruments Q800 dynamic mechanical analyzer to obtain the viscoelastic properties of damaged and undamaged GFRP specimens. The single cantilever fixture has been used for performing the DMA tests. As shown in Figure 1-d, specimens with dimensions of 35.0 × 10.0 mm^2 (length × width) were cut from failed specimens for DMA tests according to the DIC results (to cut samples with different damage states). The creep-recovery tests were carried out for 60 and 120 minutes for each loading part, respectively. In order to apply the TTSP for obtaining the viscoelastic properties, creep-recovery tests were performed in the temperature range of 25–75°C with 10°C intervals. The same testing configuration was considered for the undamaged GFRP specimens to compare the viscoelastic properties.

3. Analysis and discussion

3.1 Cycle-dependent properties

The results of the quasi-static experiments are shown in Figure 2-a. The ultimate tensile strength (UTS) was estimated as 157 ± 9 MPa. The fatigue test results were used to obtain the S-N curves for different *R*-ratios. The S-N curves were obtained by normalizing the maximum stress by the UTS resulting from quasi-static tests to exclude the scattering resulting from the ultimate strength of GFRP laminate. As shown in Figure 2-b, the S-N curves for different *R*-ratio presented with dashed lines and the fatigue experimental data shown by open symbols. As a result of the relatively large deformation of the $[\pm 45]_{2s}$ GFRP laminates under fatigue loading, the level of true stress applied during loading will increase. The effect of the true stress state on S-N curves is investigated by adjusting the stress level based on the strain evolution monitored during loading. The adjusted experimental data are presented by filled symbols and the corresponding S-N curves by solid lines in Figure 2-b. By comparison of S-N curves, it can be realized the underestimation of S-N curves, especially at higher *R*-ratios and stress levels, where creep deformation would be more considerable. As a result, the underestimation of S-N curves can lead to overdesigning of FRP composites' structures. Therefore, it is suggested to consider the true stress levels applying for fatigue tests analysis, i.e., especially to obtain the in-plane shear properties using $[\pm 45]_{2s}$ laminates for designing and also numerical modeling purposes.

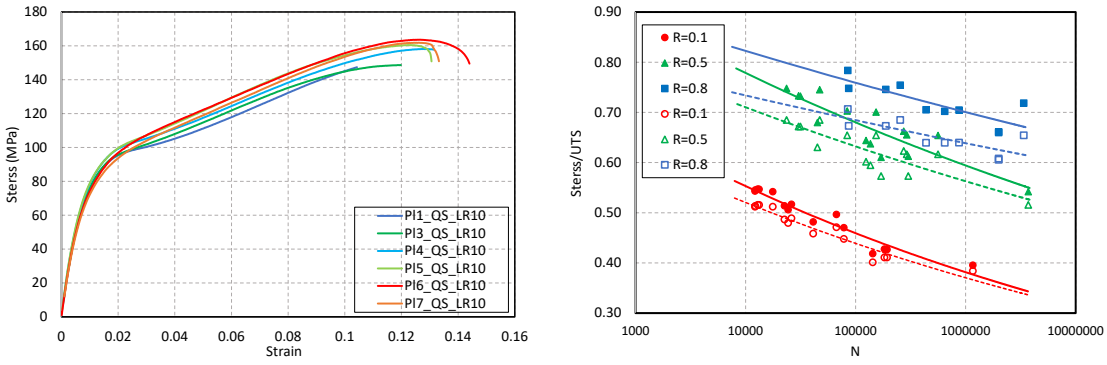

(a) (b)

Figure 2. (a) Stress-strain for same the GFRP laminates fabricated (b) S-N curves for R-ratio of 0.1, 0.5, and 0.8, before (dashed lines and unfilled shapes) and after (solid lines and filled shapes) stress adjustment due to large deformation

In the next step, the effect of fiber reorientation on the evolution of fatigue stiffness during loading has been studied. The fiber reorientation as a result of the cyclic creep (time-dependent deformation) can be estimated from the measurements of the longitudinal and traverse strains. Therefore, the average fiber reorientation in each cycle can be calculated directly by using the DIC measurements for strains in both directions. Based on the results obtained in this work, the fiber reorientation could increase up to 10 degrees for fatigue tests with the *R*-ratio of 0.8. At a higher *R*-ratio and higher maximum stress levels, the material undergoes more creep deformation, and consequently, more fiber reorientation can be experienced. Using the fiber reorientation evolution obtained during fatigue testing, the fatigue stiffness increase due to fiber reorientation can be estimated by CLT. Finally, the normalized fatigue stiffness monitored during the loading can be decomposed to the fatigue stiffness degradation due to fatigue damage and stiffening caused by fiber reorientation. The results of fatigue experiments for high and low maximum stress levels and for *R*-ratio of 0.1, 0.5 and 0.8 are shown in Figure 3. The evolution of normalized fatigue stiffness, degradation due to fatigue damage, and stiffening resulting from fiber reorientation are depicted in black, red, and blue colors, respectively. The selected fatigue tests represented high and low maximum stress levels are compared in Figure 3-a, Figure 3-b, and Figure 3-c for R=0.1, 0.5, and 0.8, respectively. The Fatigue tests reported are named with the stress level ratio (S, maximum stress level/UTS) and *R*-ratio (R). According to Figure 3-c, at a higher *R*-ratio and higher stress level (S0.71_R0.8), more effects of stiffening due to fiber reorientation can be observed. This actually results from more creep deformation, which could increase the stiffness up to 60%.

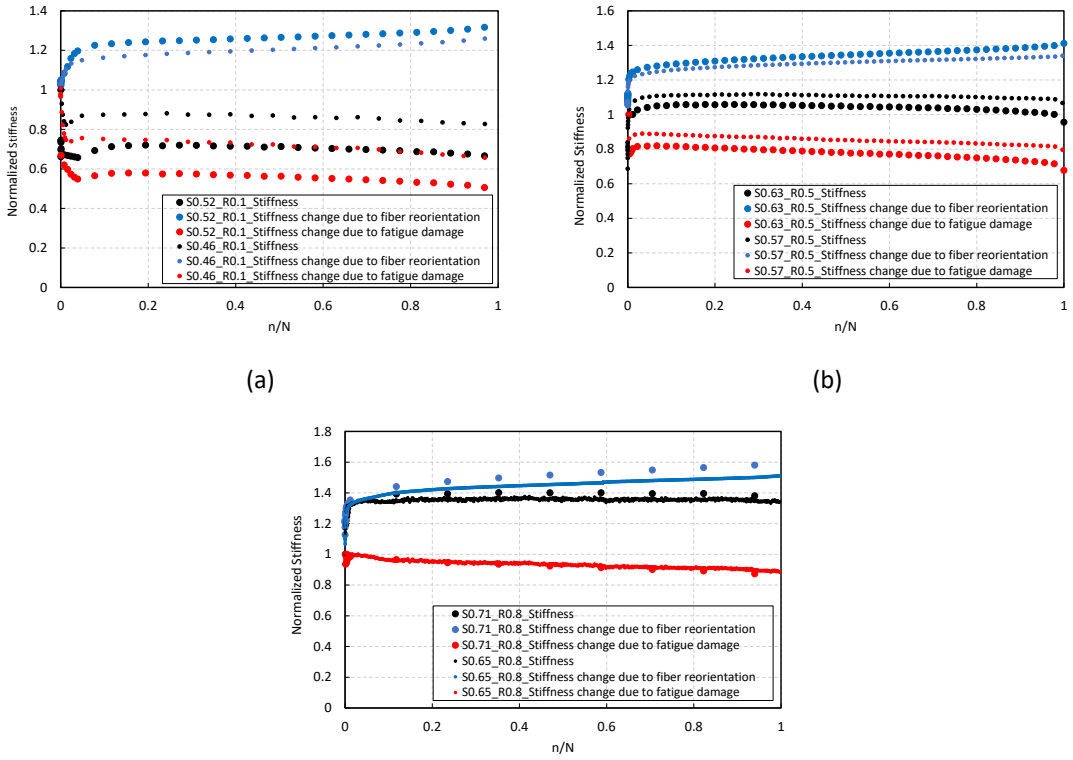

Figure 3. Decomposition of fatigue stiffness evolution due to fiber reorientation and fatigue damage for high and low maximum stress levels at different R-ratio (a) R=0.1, (b) R=0.5, and (c) R=0.8

Considering the fatigue stiffness evolution due to only fatigue damage, the residual stiffness model can be developed to interpret pure fatigue damage evolution. As shown in Figure 3, the stiffness evolution due to fatigue damage is decreasing for all fatigue tests. According to Figure 3-a, at the lower *R*-ratio of 0.1 and at higher stress level (S0.52_R0.1), where fatigue damage dominates the material behavior, the fatigue stiffness decreased, due to fatigue damage, to ca. 50%, while the decrease was less for higher *R*-ratios (See Figs3-b, 3-c), and it almost vanishes for *R*=0.8, where the creep dominates the material behavior.

3.2 Time-dependent properties

The results obtained from DMA experiments conducted on a limited amount of damaged and undamaged specimens. According to Figure 4-a, the creep strain curves were obtained for the undamaged specimen at temperatures in the range of 25–75 °C. The same DMA experimental procedure has been performed on the sample cut from the specimen that failed in the fatigue experiment of "S0.46_R0.1." The result shown in Figure 4-b corresponds to the top-left located sample (cut according to the DIC result in Figure 4-c). The creep strain curves for each damaged and undamaged test have been used to obtain the creep strain master curves using the TTSP. The shift factors have been obtained by adopting the Williams-Landel-Ferry (WLF) model [8]. The results show the feasibility of applying TTSP on damaged GFRP material to obtain the viscoelastic properties depending on the damage level caused during fatigue loading. As shown in Figure 4-c, applying TTSP on a fatigue-damaged specimen provides a smooth master curve to predict creep strain for a longer time period. As seen in Figure 4-c, the creep master curves of the damaged and undamaged specimens are comparable, with the master curve for the damaged material shifted upward at the early stages due to fatigue stiffness degradation, which affects the instantaneous strain. Besides mentioned shifting, the fatigue damage alters the viscoelastic behavior for longer periods, as the master curve diverges more from the one for the undamaged sample. As a result of this observation, extending the TTSP to the time-temperature-fatigue damage superposition principle would be suggested to predict viscoelastic properties depending on the damage level caused during loading. To validate the proposed methodology, more DMA experiments are needed for various fatigue tests performed at different stress levels and *R*-ratios. Finally, it will be possible to establish the novel creep master curves depending on the different loading conditions and the level of fatigue damage. Therefore, the proposed master curve would be used for more accurate modeling and to predict the long-term behavior of FRP composites considering both fatigue damage and creep deformation.

3.3 Damage propagation and failure modes

The DIC measurements were post-processed using the VIC-2D software (from Correlated Solutions, Inc). A field size (160 mm × 25 mm) was defined on each initial image of the samples to capture the specimen's strain field under loading. The most important parameters related to post-processing using DIC software are the subset and step size, as well as the interpolation type. The parameters were tuned effectively, corresponding to the speckle pattern created by spraying.

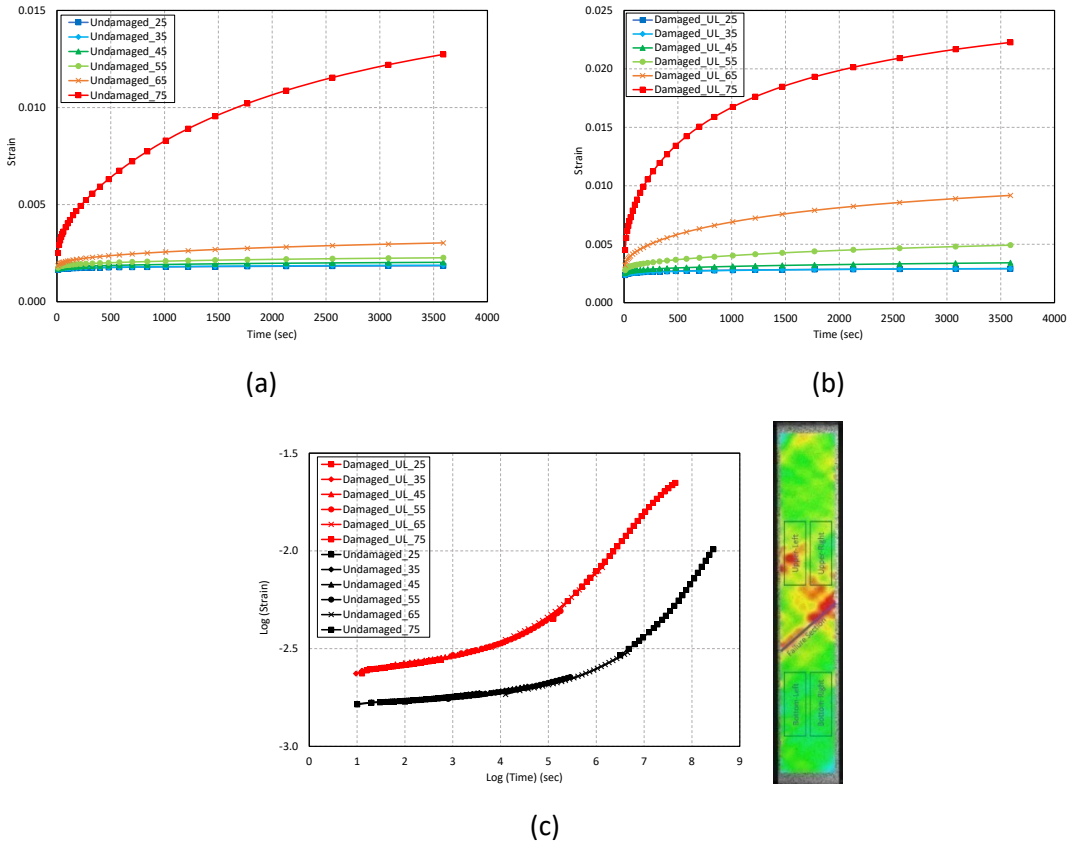

Figure 4. (a) Creep strain curves obtained from creep-recovery tests for temperatures in the range of 25–75 °C on (a) undamaged $[\pm 45]_{2s}$ GFRP, (b) Damaged specimens cut from fatigue test of S0.46_R0.1 (The top-left position in the DIC image), (c) Comparison of creep master curves obtained by TTSP for damaged (S0.46_R0.1, top-left) and undamaged material

As a result of relatively large deformation, the Hencky strain (logarithmic) was used to consider true strain. Finally, the DIC results for longitudinal strain (loading direction) are presented in Figure 5 to qualitatively compare the damage initiation and propagation under different loading conditions. First of all, compared to the IR thermography results, which are not presented here, the DIC method would provide a higher resolution to monitor different damage modes initiated and propagated during the loading. In Figure 5, the longitudinal strain field at different fractions of life is presented for *R*-ratios of 0.1 (top), 0.5 (middle) and 0.8 (bottom). For each *R*-ratio, two test results represent high (left) and low (right) stress levels. By comparing the longitudinal strain distribution, it can be realized that under a lower *R*-ratio (0.1), where fatigue dominates the material behavior, the damage is more concentrated. However, under the *R*-ratio of 0.8 (creep-dominated), the strain distribution and damage distribution are more uniform throughout the specimen. The damage was initiated mainly by matrix cracking at the free edges at the early stages of fatigue loading. In the next stage, the micro-cracks initiated could be propagated parallel to the fiber directions as macro matrix cracks or fiber/matrix debonding. Finally, the propagated damages would mostly lead to delamination and fiber breakage causing the failure of the laminate. Selected images of failure surfaces for different *R*-ratios are presented in Figure 6. The results show different failure modes as fiber breakage, mixed fiber breakage/pull-out, and fiber pull-out for *R*-ratios of 0.1, 0.5 and 0.8, respectively.

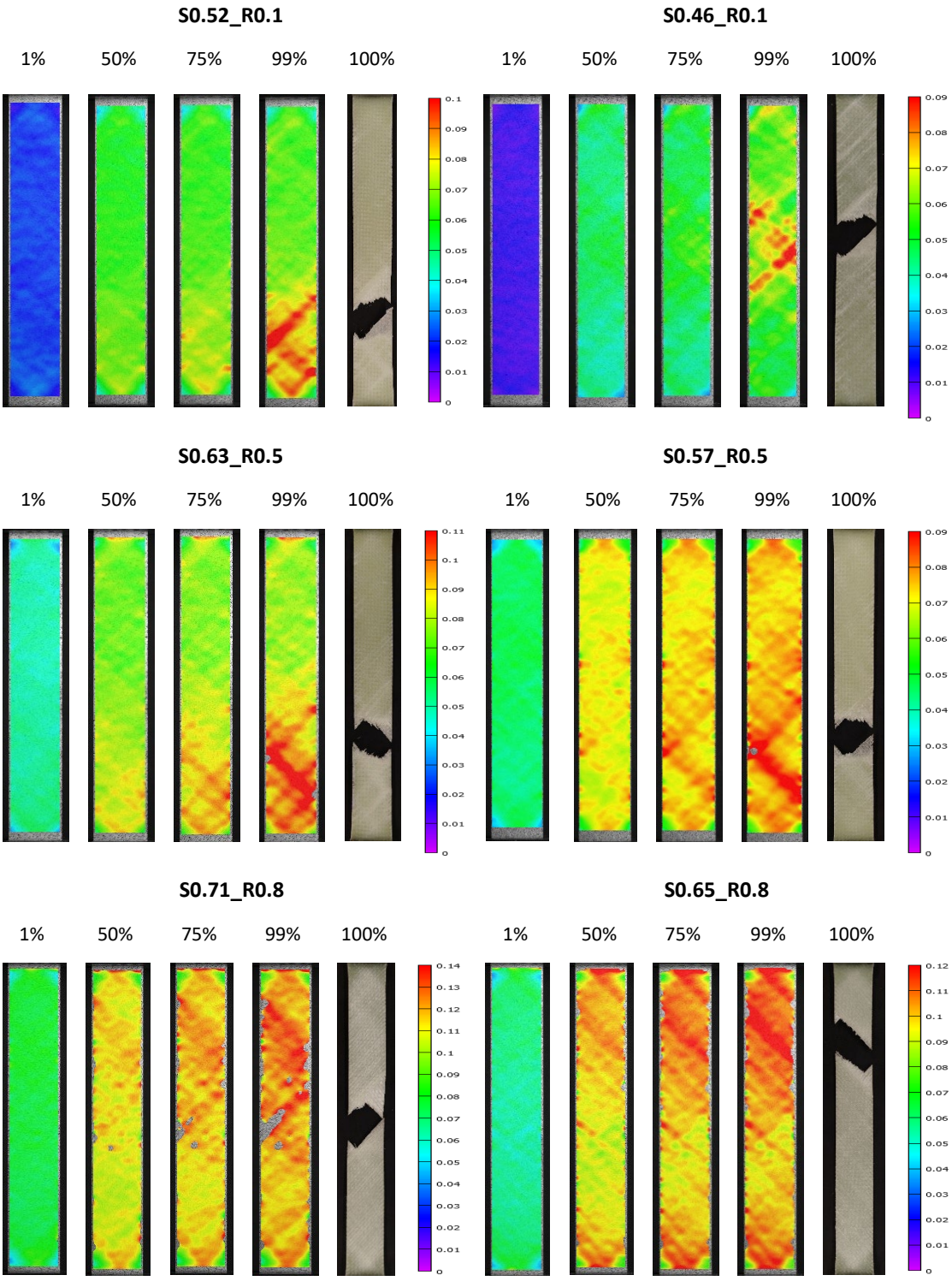

Figure 5. The DIC measurements for longitudinal strain during fatigue tests for R-ratios of 0.1 (top), 0.5 (middle) and 0.8 (bottom), and under high (left) and low (right) stress levels

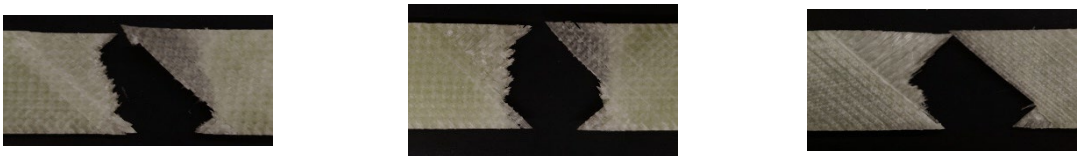

(a) S0.52_R0.1: Fiber breakage (b) S0.57_R0.5: fiber breakage/pull-out (c) S0.71_R0.8: Fiber pull-out

Figure 6. The dominant failure modes under different R-ratios: (a) 0.1, (b) 0.5, (c) 0.8

4. Conclusion

The fatigue behavior of angle-ply GFRP laminates was studied considering time- and cycle-dependent behaviors. Different aspects of their interactions under tension-tension CA fatigue loading were addressed. For cycle-dependent properties, it has been shown that the S-N curves were underestimated due to the increasing stress state under fatigue loading, i.e., resulting from large creep deformation, especially for higher *R*-ratio and stress levels. Moreover, the effect of fiber orientation on fatigue stiffness evolution was investigated. A simple analysis was performed to decompose the stiffening effect due to fiber orientation from the fatigue damage stiffness evolution, which provides more accurate residual stiffness models representing the pure fatigue degradation. An experimental methodology using DMA testing was suggested to evaluate the effect of fatigue damage on viscoelastic properties. The results have shown the feasibility of using the time-temperature superposition principle for damaged material, which can provide viscoelastic properties depending on the fatigue damage level. Since limited results were used in this work, the DMA testing should be performed for more damaged specimens under different loading conditions to evaluate the performance of the proposed methodology. Finally, the evolution of DIC measurements and failure surfaces have been discussed for different loading conditions. As a result, it can be concluded that depending on the *R*-ratio, the damage distribution and failure modes could differ, resulting from different inherent behavior of FRP composite materials under creep and fatigue loading.

Acknowledgements

The authors wish to acknowledge the support and funding of this research by the Swiss National Science Foundation (Grant No. 200020_185005).

5. References

1. Anastasios P. Vassilopoulos, Keller T. Fatigue of Fiber-Reinforced Composites. Springer Science & Business Media; 2011.
2. Anastasios P. Vassilopoulos. The history of fiber-reinforced polymer composite laminate fatigue. Int J Fatigue. 2020;134:105512.
3. A. Vahid Movahedi-Rad, Anastasios P. Vassilopoulos, Thomas Keller. Creep effects on tension-tension fatigue behavior of angle-ply GFRP composite laminates. Int J Fatigue. 2019;123:144–56.
4. A. Vahid Movahedi-Rad, Thomas Keller, Anastasios P. Vassilopoulos. Interrupted tension-tension fatigue behavior of angle-ply GFRP composite laminates. Int J Fatigue. 2018 Aug 1;113:377–88.
5. Samareh-Mousavi SS, Taheri-Behrooz F. A novel creep-fatigue stiffness degradation model for composite materials. Compos Struct. 2020 Apr 1;237:111955.
6. Reddy JN. Mechanics of laminated composite plates and shells: theory and analysis. CRC Press; 2003.
7. Williams ML, Landel RF, Ferry JD. The Temperature Dependence of Relaxation Mechanisms in Amorphous Polymers and Other Glass-forming Liquids. J Am Chem Soc. 1955;77(14):3701–7.
8. Povolo F, Fontelos M. Time-temperature superposition principle and scaling behaviour. J Mater Sci 1987 225. 1987 May;22(5):1530–4.

